Natural convection in enclosures containing an insulation with a permeable fluid-porous interface

S. B. Sathe, W.-Q. Lin, and T. W. Tong
Department of Mechanical and Aerospace Engineering,
Arizona State University, Tempe, AZ 85287, USA

Received June 1987 and accepted for publication February 1988

A numerical study was performed to analyze steady-state natural convective heat transfer in rectangular enclosures vertically divided into a fluid-filled region and a fluid saturated porous region. The interface between the two regions was permeable, allowing the fluid to flow from one region to the other. The vertical boundaries of the enclosures were isothermal and the horizontal boundaries were adiabatic. The flow in the porous region was modeled using the Brinkman-extended Darcy's law to account for no-slip at the walls and the interface. Numerical experiments were performed for different enclosure aspect ratios, Rayleigh numbers, Darcy numbers, thermal conductivity ratios and thicknesses of the porous region. The effects of the governing parameters on heat transfer were established. It was found that, when compared to the case where the fluid and porous regions were separated by an impermeable partition, heat transfer across the enclosure was higher. Also, for certain values of the governing parameters, heat transfer across the enclosure could be minimized by filling the enclosure partially with a porous material instead of filling it entirely.

Keywords: natural convection; porous medium; permeable interface; enclosure; insulation

Introduction

Natural convection in enclosures has been studied extensively[1–17] due to its applications in many engineering systems. In a recent study pertaining to thermal insulation applications, Tong and Subramanian[15] studied the effect of filling a vertical rectangular enclosure partially with a porous medium. The porous and fluid regions were considered to be separated by an impermeable partition. It was found that there were conditions where heat transfer exhibited a minimum as the porous thickness was increased from zero to the enclosure width.

The present work examines the case where there is no partition separating the fluid and porous regions. Such a situation arises in the use of unfaced fiberglass batts. The fluid flow characteristics in the enclosure are quite different from those for the previous case[15] as the fluid in one region can now flow into the other. Consequently, the rate of heat transfer across the enclosure can also be quite different.

In a study motivated by an interest in material castings, Beckermann *et al.*[17] have also studied heat transfer in an enclosure containing a fluid-porous interface. They conducted a detailed analysis on the heat and fluid flow characteristics between the porous and fluid regions, but considered only the case for enclosures with an aspect ratio of 1. Since most insulation systems are tall and narrow, attention of the present work is focused on the cases with an aspect ratio of 5 or larger. The effect of the absence of an impermeable partition will be established by comparing the results to those presented by Tong and Subramanian.[15] Also, the question whether heat transfer can still be minimized as a function of the thickness of the porous region will be addressed.

Mathematical formulation

Figure 1 shows the geometry, boundary conditions and the coordinate system for the problem under consideration. The enclosure has a height L and a width d. The interface is permeable, allowing the fluid to flow from one region to the other. The porous medium is completely saturated with the fluid and is assumed to be macroscopically isotropic, homogeneous, and in local thermal equilibrium. The thermophysical

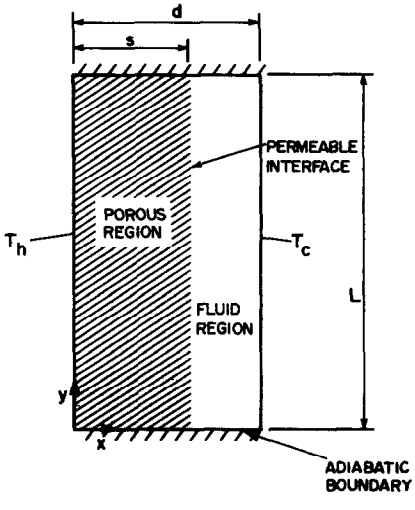

Figure 1 Enclosure partially filled with a porous medium

properties of both the fluid and the porous medium are assumed constant except for the fluid density in the buoyancy term of the momentum equation. The fluid flow is assumed to be two-dimensional, steady-state, laminar, and incompressible.

In the porous region Brinkman-extended Darcy's formulation is used so that the no-slip condition at the walls and interface can be satisfied. The convection terms are retained to account for the inertia of the fluid. The equations governing momentum and energy transfer can be written in dimensionless form as

Porous region

$$U_p \frac{\partial \Omega_p}{\partial X} + V_p \frac{\partial \Omega_p}{\partial Y} = -\frac{\mathrm{Pr}}{\mathrm{Da}} \Omega_p + \mathrm{Pr}\, \nabla^2 \Omega_p + \mathrm{RaPr} \frac{\partial \theta_p}{\partial X} \tag{1}$$

$$\nabla^2 \psi_p = -\Omega_p \tag{2}$$

$$U_p \frac{\partial \theta_p}{\partial X} + V_p \frac{\partial \theta_p}{\partial Y} = \frac{\nabla^2 \theta_p}{R_c} \tag{3}$$

Fluid region

$$U_f \frac{\partial \Omega_f}{\partial X} + V_f \frac{\partial \Omega_f}{\partial Y} = \mathrm{Pr}\, \nabla^2 \Omega_f + \mathrm{PrRa} \frac{\partial \theta_f}{\partial X} \tag{4}$$

$$\nabla^2 \psi_f = -\Omega_f \tag{5}$$

$$U_f \frac{\partial \theta_f}{\partial X} + V_f \frac{\partial \theta_f}{\partial Y} = \nabla^2 \theta_f \tag{6}$$

where ∇^2 is the Laplacian operator and the symbols are defined in the Notation. The assumption $\mu_p = \mu_f$[18] has been invoked and the following dimensionless variables have been used in arriving at Equations 1 through 6 from their original dimensional form

$$X = \frac{x}{d}, \quad Y = \frac{y}{d}, \quad \theta = \frac{T - T_c}{T_h - T_c}$$

$$U_p = \frac{u_p d}{\alpha_f}, \quad V_p = \frac{v_p d}{\alpha_f}, \quad U_f = \frac{\mu_f d}{\alpha_f}, \quad V_f = \frac{v_f d}{\alpha_f}$$

$$\mathrm{Ra}_0 = \frac{\rho g \beta (T_h - T_c) \kappa d}{\mu_f \alpha_p}, \quad \mathrm{Ra} = \frac{\rho g \beta (T_h - T_c) d^3}{\mu_f \alpha_f}$$

$$\mathrm{Da} = \frac{\kappa}{d^2}, \quad \mathrm{Pr} = \frac{\mu_f}{\rho \alpha_f}$$

The dimensionless stream function and vorticity are defined as

$$U = \frac{\partial \psi}{\partial Y}, \quad V = -\frac{\partial \psi}{\partial X}, \quad \Omega = \frac{\partial V}{\partial X} - \frac{\partial U}{\partial Y} = \nabla^2 \psi$$

The boundary conditions are

at $X = 0$ $\quad \theta_p = 1, \quad \psi_p = \frac{\partial \psi_p}{\partial X} = 0, \quad \Omega_p = -\nabla^2 \psi_p$

at $X = 1$ $\quad \theta_f = \psi_f = \frac{\partial \psi_f}{\partial X} = 0, \quad \Omega_f = -\nabla^2 \psi_f$

at $Y = 0, A$ $\quad \frac{\partial \theta_p}{\partial Y} = \psi_p = \frac{\partial \psi_p}{\partial X} = 0, \quad \Omega_p = -\nabla^2 \psi_p$ for $X < S$

$\frac{\partial \theta_f}{\partial Y} = \psi_f = \frac{\partial \psi_f}{\partial X} = 0, \quad \Omega_f = -\nabla^2 \psi_f$ for $X > S$

where $A = L/d$ and $S = s/d$. At the interface, the following quantities evaluated in both the porous and fluid regions are matched: horizontal velocity, vertical velocity, shear stress, normal stress, temperature, and heat flux. Mathematically, these matching conditions can be expressed as

$$\psi_p = \psi_f, \quad \frac{\partial \psi_p}{\partial X} = \frac{\partial \psi_f}{\partial X}$$

$$\Omega_p = \Omega_f, \quad \frac{\partial \Omega_p}{\partial X} - \frac{V_p}{\mathrm{Da}} = \frac{\partial \Omega_f}{\partial X} \tag{7}$$

$$\theta_p = \theta_f, \quad \frac{\partial \theta_p}{\partial X} = R_c \frac{\partial \theta_f}{\partial X}$$

Notation

A	Aspect ratio of enclosure, L/d
d	Enclosure width
Da	Darcy number, κ/d^2
g	Acceleration due to gravity
k	Thermal conductivity
L	Height of enclosure
$M1$	Number of intervals in the porous region in the x direction
$M2$	Number of intervals in the fluid region in the x direction
N	Number of intervals in the y direction
Nu	Nusselt number
p	Pressure
Pr	Prandtl number, $\mu_f/\rho\alpha_f$
R	R_c in porous region; 1 in fluid region
R_c	Ratio of k_f to k_p
Ra	Rayleigh number, $\rho g \beta_f (T_f - T_c) d^3/\mu_f \alpha_f$
Ra_0	Modified Rayleigh number, $\mathrm{RaDa}R_c$
s	Width of the porous region
S	Dimensionless width of the porous region, s/d
T	Temperature
u	Horizontal velocity
U	Dimensionless horizontal velocity, ud/α_f
v	Vertical velocity
V	Dimensionless vertical velocity, vd/α_f
x	Horizontal coordinate
X	Dimensionless horizontal coordinate, x/d
y	Vertical coordinate
Y	Dimensionless vertical coordinate, y/d
α	Thermal diffusivity
β	Coefficient of volumetric expansion
Γ	Parameter in Equation 10
ζ	Parameter in the source function in Equation 10
η	Parameter in the source function in Equation 10
θ	Dimensionless temperature, $(T - T_c)/(T_h - T_c)$
κ	Permeability
μ	Dynamic viscosity
ρ	Density of the fluid
ϕ	Intensive variable in Equation 10
ψ	Dimensionless stream function
ω	Underrelaxation parameter
Ω	Dimensionless vorticity

Subscripts

c	Cold wall
f	Fluid
h	Hot wall
m	Mean
p	Porous medium

where $R_c = k_f/k_p$. Note that Ra_0, Ra, Da, and R_c are related by

$$Ra_0 = RaDaR_c \tag{8}$$

and hence only three of these parameters are independent.

The heat transfer results are presented in terms of the Nusselt number (Nu), defined as the ratio of the actual heat transfer across the enclosure to the heat transfer by conduction when the entire enclosure is filled with the fluid only. In terms of the variables, it is

$$Nu(x) = -\frac{1}{AR}\int_0^A \left(\frac{\partial\theta}{\partial X} - \theta U\right) dY \tag{9}$$

where

$$R = R_c, \quad \theta = \theta_p, \quad U = U_p \quad \text{for } X \leqslant S$$

$$R = 1, \quad \theta = \theta_f, \quad U = U_f \quad \text{for } X \geqslant S$$

Method of solution

Equations 1 through 6 were solved numerically using a finite-difference method. The momentum and energy equations were expressed in a canonical form as follows[19]:

$$\frac{\partial}{\partial X}\left[U\phi - \Gamma\frac{\partial\phi}{\partial X}\right] + \frac{\partial}{\partial Y}\left[V\phi - \Gamma\frac{\partial\phi}{\partial Y}\right] = \zeta\phi + \eta \tag{10}$$

This form of two-dimensional equation describes the conservation of any intensive dimensionless property ϕ in the control volume approach. The respective velocities in X and Y directions are U and V, and $\zeta\phi + \eta$ is a linear source term. Equations 1, 3, 4, and 6 were cast into the above form with ϕ corresponding to either Ω or θ and Γ corresponding to either Pr or $1/R_c$, respectively. There is no source term in the energy equation. The source term in the momentum equation for the porous region is a combination of the Darcy resistance and buoyancy terms with ζ and η representing $-\mathrm{Pr/Da}$ and RaPr, respectively. The source term for the fluid region consists of the buoyancy term only and η corresponds to RaPr. The partial derivatives at the interior nodes were discretized by using the mesh control volume scheme and the power law.[19] The power-law scheme is used because it has been shown to predict the heat and fluid flow characteristics in a very realistic manner for all ranges of grid Peclet numbers.

The momentum, energy and the ψ-Ω equations were solved using the Gauss-Seidel iterative method. The discretized difference equations were arranged in a tridiagonal matrix form. The Thomas algorithm[20] and line-by-line scheme[21] were employed to solve the equations for the downstream values. Different expressions for the vorticity at the boundary have been examined in the past.[22] Here a second order expression was adapted,

$$\Omega_i = \frac{7\psi_i - 8\psi_{i+1} + \psi_{i+2}}{2(\Delta n^2)} + O(\Delta n^2)$$

where i denotes the boundary node and Δn is the spatial interval in the direction normal to the boundary.

The entire enclosure was divided into a $(M1 + M2) \times N$ uniform grid system. $M1$ and $M2$ are the numbers of intervals in the X direction in the porous and fluid regions, respectively, and N is the number of intervals along the Y direction. The stagnant conditions were used as the initial guess and θ, ψ, and Ω were iterated at every grid point until covergence was obtained. For higher Ra, the values of θ, ψ, and Ω for lower Ra were used as the initial guess to achieve faster convergence. The convergence criterion was set such that the iterations continued until the change in θ, ψ, and Ω at all the grid points was less than 0.01%.

All the results presented are for a $(24+24) \times 32$ grid. It was found that after halving the mesh size (using a $(48+48) \times 64$ grid) the Nusselt numbers changed by less than 2.5%. The Nusselt numbers at the hot wall, cold wall and the interface were examined for energy balance and they were found to be within 0.5% of one another in all of the cases considered. The Nusselt numbers to be presented are those for the hot wall.

A word should be added about the overall numerical stability. Although the power law is stable for a single region problem (i.e., pure fluid region or pure porous region), the overall numerical iteration may be unstable due to the introduction of the matching conditions at the interface. A permeable interface introduces the Darcy resistance, V/Da, in one of the interface matching conditions, Equation 7. For $\mathrm{Da} < 10^{-5}$, this term becomes large enough to cause numerical instability. Thus, for Da lower than 10^{-5}, substantial underrelaxation had to be employed for Equation 7 so that

$$\Omega_i^{n+1} = \omega\Omega_i^{n+1/2} + (1-\omega)\Omega_i^n, \qquad \omega = 0.1$$

where $n+1/2$ signifies an intermediate value before relaxation, ω denotes an underrelaxation parameter and i denotes the interface node. It was found that increasing underrelaxation parameter for Ω_i to 0.5 resulted in significantly faster convergence at values of Da higher than 10^{-5}.

Results and discussion

The governing parameters are Ra, Da, A, R_c, S, and Pr. The value 0.7 was used for Pr for all the calculations. This value approximates that for air at room temperature. Different values for the other parameters were used in order to establish their effects. Before the results are presented, the comparisons conducted to validate the computer code will be examined.

Comparisons with other results

Table 1 shows the comparison of Nu for various values of S. The results for $S = 0$ (Table 1(a)) agree to within 5% with those presented by Tong and Subramanian.[15] The differences are attributed to the different discretization methods and the different grid sizes employed. Tong and Subramanian[15] used central differences and larger grid sizes. The agreement with the results by Raithby and Wong[6] is better than 1% except the case for $A = 10$ and $\mathrm{Ra} = 1 \times 10^5$ where the agreement is 3%. Beckermann *et al.*[17] have analyzed a similar problem for the case of $A = 1$. The comparison with their results (Table 1(b)) for $S = 0.25$, 0.5, and 0.75 show agreements within 7%. Beckermann *et al.*[17] presented their results in a graph and some errors might have been introduced in reading the graph. For $S = 1$, the comparison is in Table 1(c). The present results match with those of Tong and Subramanian[15] better than 4%. Note that the results from Shiralkar *et al.*[13] are for pure Darcy formulation and hence their Nu are all higher (by about 3%) than the present values.

Comparisons with experimental results

Experimental measurements were also conducted to validate the present numerical model. The experiments were conducted by Tong and Sathe as a continuation of a previous study[16] for natural convection in partially porous enclosures with an impermeable partition separating the fluid and porous regions. The experiments were carried out in exactly the same fashion as described in Ref. 16 except that the impermeable partition was removed from the enclosure. A foam plastic was used as the porous material and distilled water was used as the fluid. Flow visualization was performed by seeding the fluid region with shiny natural pearl essence particles and shining a narrow beam

Table 1 Comparison of Nu: (a) $S=0$, $Da=10^{-3}$, $R_c=1$; (b) $A=1$, $Ra=10^5$, $Da=10^{-3}$, $R_c=1$; and (c) $S=1$, $Da=10^{-3}$, $R_c=1$

		Nu		
A	$Ra\times10^{-4}$	Present	Tong and Subramanian[15]	Raithby and Wong[8]
5	1	1.987	1.945	2.00
5	10	3.714	3.580	3.68
10	1	1.681	1.614	1.67
10	10	3.230	3.067	3.13

(a)

	Nu	
S	Present	Beckermann *et al.*[17]
0.25	3.604	3.4
0.50	3.348	3.2
0.75	3.101	2.9

(b)

		Nu		
A	Ra_0	Present	Tong and Subramanian[15]	Shiralkar *et al.*[13]
5	50	1.459	1.42	
5	100	2.033	1.95	2.09*
10	50	1.213	1.20	1.25*
10	100	1.524	1.48	1.57*

* Based on pure Darcy formulation, i.e., $Da=0$.

(c)

Table 2 Comparison with experimental results: $A=5$, $Da=3.674\times10^{-4}$, $S=0.5$, $R_c=1.01$

		Nu	
$Ra\times10^{-5}$	Pr	Present numerical	Experimental
6.01	6.72	3.796	3.52
4.03	6.53	3.224	3.34
3.33	6.82	2.986	2.81

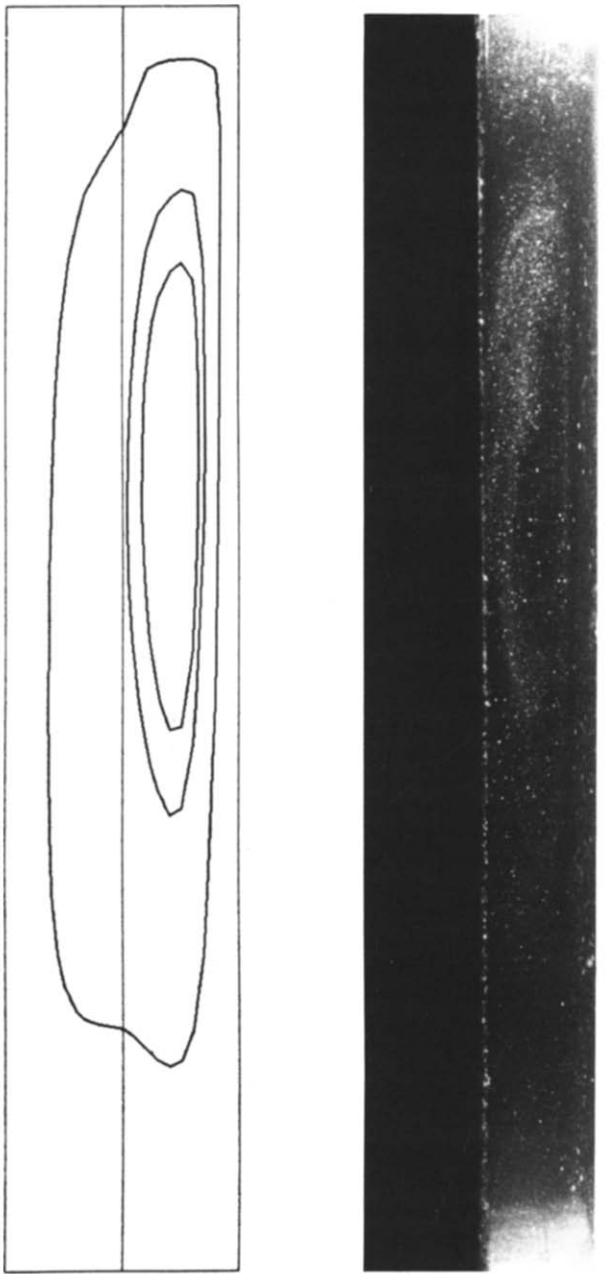

Figure 2(a) Comparison of the predicted streamlines with photographed flow pattern for $A=5$, $R_c=1.01$, $Da=3.674\times10^{-4}$, $S=0.5$, $Ra=6.01\times10^5$, and $Pr=6.72$

of light through a slit from the top of the enclosure. The predicted streamlines and the actual flow pattern are presented in Figure 2. There is a good qualitative agreement between the calculated and experimentally observed flow patterns. Shown in Table 2 are the predicted and experimentally measured Nu. The agreement ranges from 4 to 7%. Based on the comparisons presented, it was concluded that the numerical model could accurately predict heat and fluid flow in partially porous enclosures with a permeable interface.

Effect of Ra

Attention is now given to the effects of the governing parameters. Plots of Nu versus S are used to illustrate these effects. Demonstrated in Figure 3 is the effect of Ra for $A=5$. As expected, higher Ra result in higher Nu. For a given Ra, the resistance to the flow increases as S is increased. The intensity of convection is reduced and results in lower Nu. For $Ra=10^5$ and $Ra=10^6$, the reduction in Nu for S increasing from 0.3 to 0.8 is very small, indicating no appreciable gain in insulation effect for these conditions. For $Ra=10^3$, almost all the convection is suppressed when $S\geqslant0.3$.

Effect of A

As illustrated in Figure 4, Nu decreases as A increases. This is a result of increasing slenderness that has the effect of suppressing convective motion. As noted before, Nu remain almost constant when S is between 0.3 and 0.8. This flat portion of the curve spans over a smaller range of S as A increases.

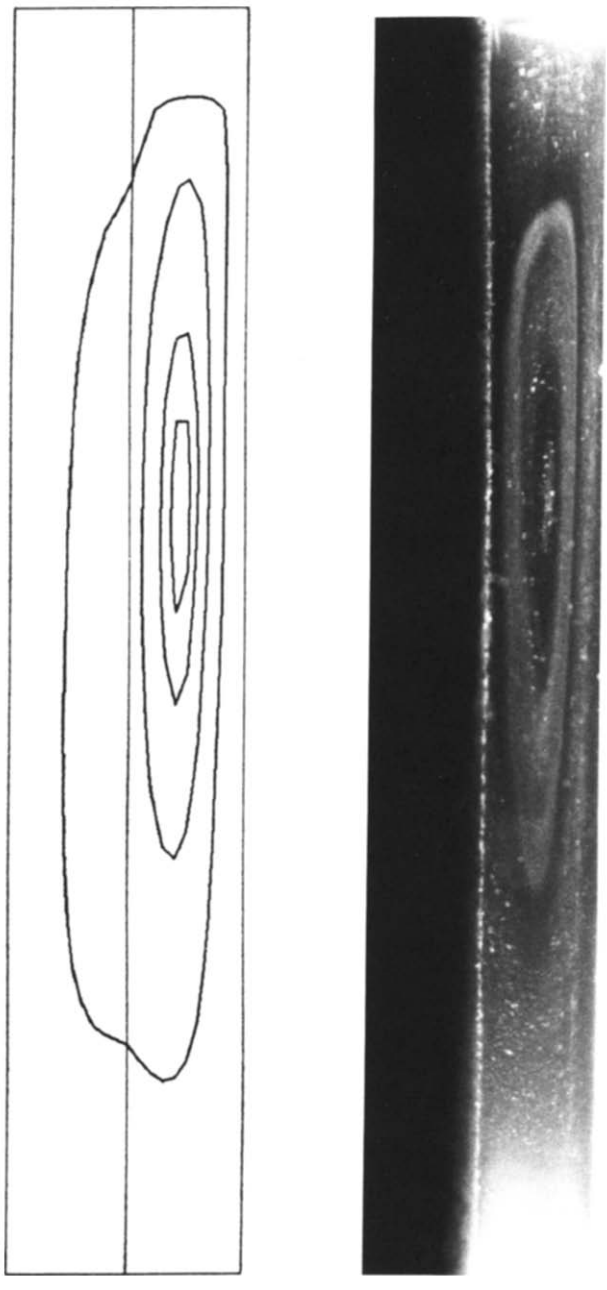

Figure 2(b) Comparison of the predicted streamlines with photographed flow pattern for $A=5$, $R_c=1.01$, $Da=3.674\times10^{-4}$, $S=0.5$, $Ra=3.33\times10^{8}$, and $Pr=6.82$

Effect of Da

Figure 5 shows Nu versus S for various Da. Changing Da from 10^{-2} to 10^{-3} and from 10^{-3} to 10^{-4} produces a larger drop in Nu as compared to changing Da from 10^{-4} to 10^{-5}. For $Da=10^{-5}$ almost all the convection is suppressed when $S\geqslant0.7$.

Effect of R_c

Shown in Figure 6 is Nu versus S for various R_c. For a given A, Nu depends on the intensity of convection in the enclosure and R_c. The intensity of convection decreases monotonically as S is increased from 0 to 1, owing to increasing resistance to flow. When $R_c>1$ or $R_c=1$, conduction through the enclosure decreases or remains the same respectively, as S changes from

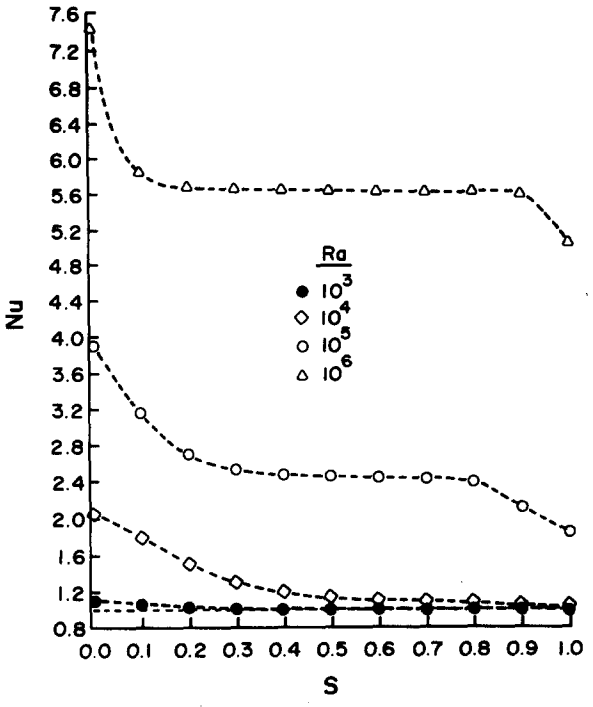

Figure 3 Effect of Ra on the variation of Nu versus S for $A=5.0$, $Da=10^{-3}$, $R_c=1$

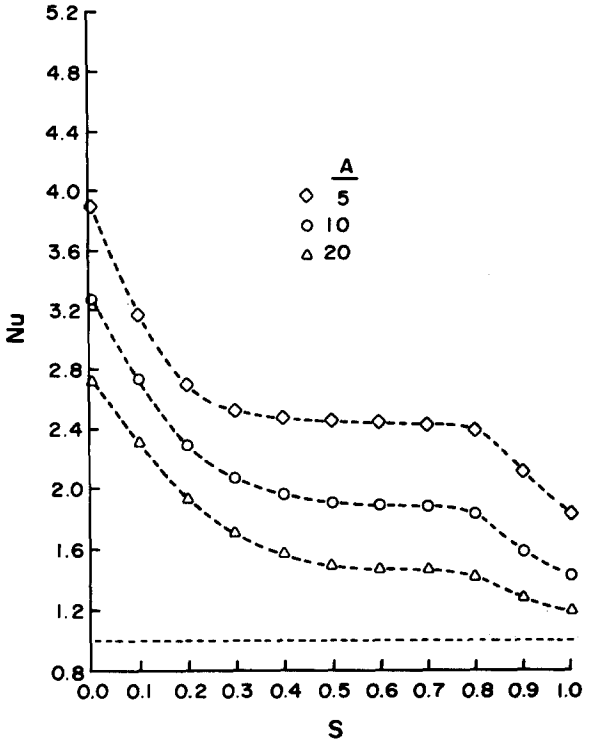

Figure 4 Effect of A on the variation of Nu versus S for $Ra=10^{8}$, $R_c=1$, $Da=10^{-3}$

0 to 1. Therefore, the combined effect of convection and conduction is a monotonic decrease in the total heat transfer when $R_c\geqslant1$. However, as shown in the figure, a minimum in the total heat transfer is possible if $R_c<1$. This is because the fluid is being replaced by a better conducting material as S increases. The minimum occurs when the decrease in convection

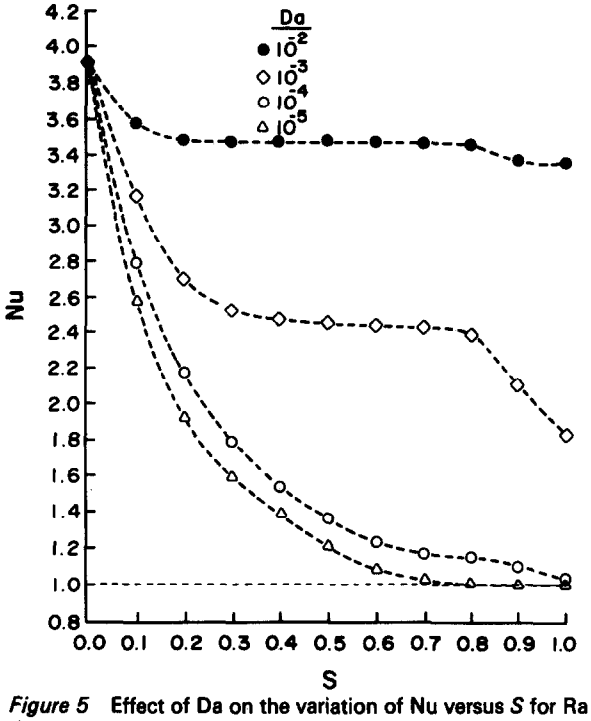

Figure 5 Effect of Da on the variation of Nu versus S for $Ra=10^5$, $A=5$, $R_c=1$

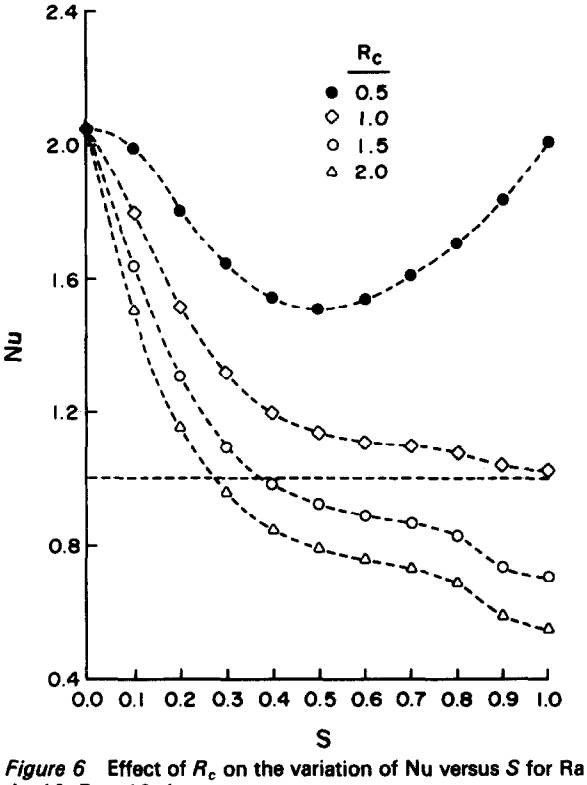

Figure 6 Effect of R_c on the variation of Nu versus S for $Ra=10^4$, $A=10$, $Da=10^{-4}$

is offset by the increase in conduction. Note that in real situations the fluid is usually a gas and consequently, R_c falls in range of one or less. The results for $R_c>1$ are included primarily for completeness.

Permeable versus impermeable interface

Figures 7 and 8 show a comparison with the results obtained earlier for a partially porous enclosure with an impermeable interface.[15] The heat transfer across the enclosure is quite different for the two cases shown except at the limiting cases of $S=0$ or 1. As expected, the Nu for enclosures with an impermeable partition is always lower than that for enclosures with a permeable interface. Note that for the conditions considered, Nu exhibited a minimum for the case of impermeable interface. The reason for the occurrence of a minimum Nu when the interface is impermeable has been given elsewhere.[15]

Critical R_c

As already demonstrated, heat transfer across the enclosure may be minimized as a function of S when $R_c<1$. However, the condition $R_c<1$ is a necessary but insufficient condition for minimizing heat transfer as a function of S. By using a half-interval search method with an accuracy of ± 0.00625, the critical R_c for $Pr=0.7$ and different combinations of Ra, Da, and A have been determined and presented in Table 3. For a given set of Ra, A, and Da, a minimum Nu can be realized if the actual R_c is less than the critical R_c shown in the table. It should be noted that low Da and low Ra results in critical R_c close to 1, while high Da and high Ra produces smaller R_c. For the same Ra and Da the critical R_c for $A=10$ is larger than that for $A=5$.

Conclusions

Natural convective heat transfer in two-dimensional rectangular enclosures has been studied. The enclosures were partially filled with a vertical porous layer, and had isothermal vertical and adiabatic horizontal walls. The fluid-porous interface was permeable. The governing equations were solved using a power-law finite-difference method.

The present numerical results agreed well with experimental results and with those available in the literature. The Nu for wide ranges of Ra, Da, and A have been obtained. The results

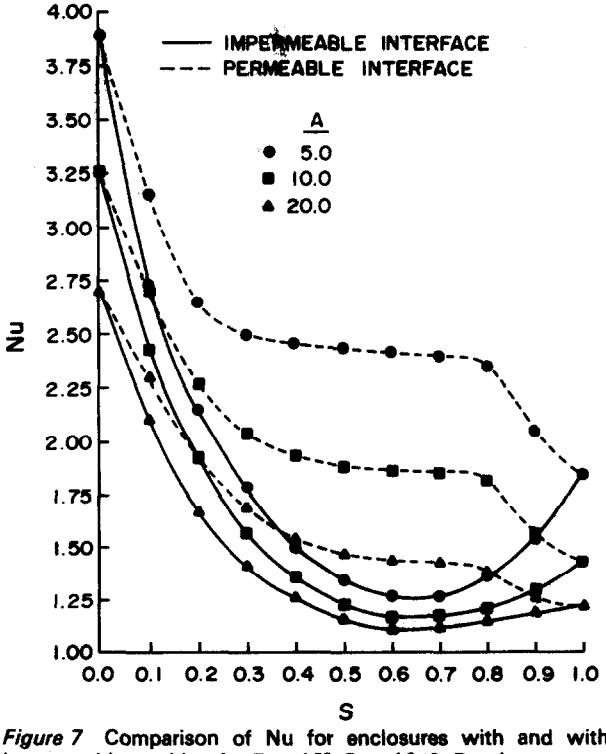

Figure 7 Comparison of Nu for enclosures with and without impermeable partition for $Ra=10^5$, $Da=10^{-3}$, $R_c=1$

Table 3 Critical R_c

		Critical R_c						
A	Da	Ra = 1×10^3	5×10^3	1×10^4	5×10^4	1×10^5	5×10^5	1×10^6
5	1×10^{-3}	0.99375	0.95625	0.88125	0.64375	0.54375	0.53125	0.53125
	1×10^{-4}	0.99375	0.99375	0.98125	0.86875	0.70625	0.55625	0.54375
	1×10^{-5}	0.99375	0.99375	0.99375	0.98750	0.98125	0.80625	0.59375
10	1×10^{-3}	0.99375	0.99375	0.88750	0.66875	0.56875	0.55000	0.54375
	1×10^{-4}	0.99375	0.99375	0.98750	0.98750	0.84375	0.58750	0.56875
	1×10^{-5}	0.99375	0.99375	0.99375	0.99375	0.99375	0.90000	0.73750

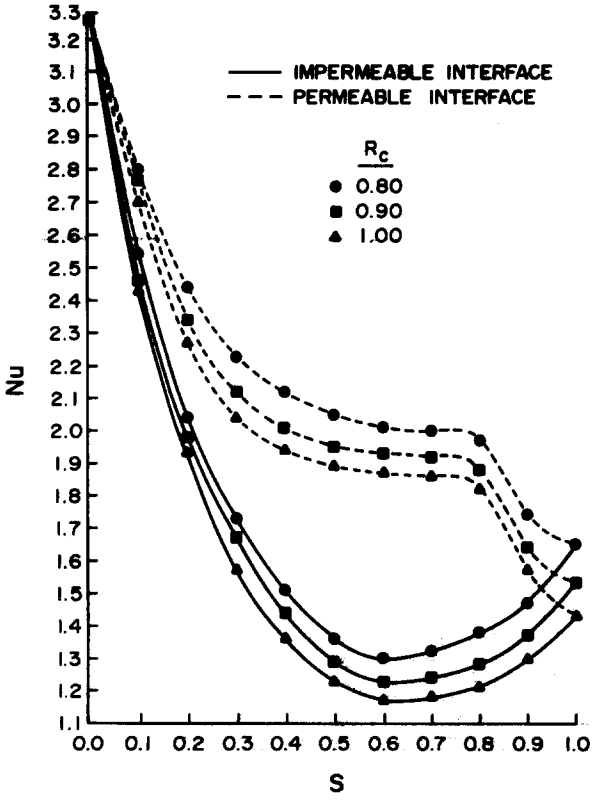

Figure 8 Comparison of Nu for enclosures with and without impermeable partition for Ra = 10^5, Da = 10^{-3}, $A = 10$

showed considerably higher rate of heat transfer when compared with those for the porous and fluid regions separated with an impermeable partition. It was found that for certain values of the governing parameters heat transfer across the enclosure could be minimized by partially filling the enclosure with a porous material, indicating a better optimized insulation usage is possible. By using a half-interval search method, the critical values of R_c for the existence of a minimum Nu were determined.

Acknowledgment

The support of this work by the National Science Foundation under grant MEA 86-96062 is appreciated.

References

1 Elder, J. W. Numerical experiments with free convection in a vertical slot. *J. Fluid Mechanics*, 1966, **24**, 823–843
2 Wilkes, J. O. and Churchill, S. W. The finite-difference computation of natural convection in a rectangular enclosure. *A.I.Ch.E.J.*, 1966, **12**, 161–166
3 Newell, M. E. and Schmidt, F. W. Heat transfer by laminar natural convection within rectangular enclosures. *J. Heat Transfer*, 1970, **92**, 159–168
4 MacGregor, R. K. and Emery, A. F. Free convection through vertical plane players—moderate and high Prandtl number fluids. *J. Heat Transfer*, 1969, **91**, 391–403
5 Ostrach, S. Natural convection in enclosures. *Advances in Heat Transfer*, 1972, **8**, 161–227
6 Raithby, G. D. and Wong, H. H. Heat transfer by natural convection across vertical air layers. *Numerical Heat Transfer*, 1981, **4**, 447–457
7 Bankvall, C. G. Natural Convective Heat Transfer in Insulated Structures. Lund Institute of Technology Report, 38, 1972
8 Chang, B. K. C., Ivey, C. M. and Barry, J. M. Natural convection in enclosed porous media with rectangular boundaries. *J. Heat Transfer*, 1970, **92**, 21–27
9 Burns, P. J., Chow, L. C. and Tien, C. L. Convection in a vertical slot filled with porous insulation. *Int. J. Heat Mass Transfer*, 1977, **20**, 919–926
10 Walker, K. L. and Homsy, G. M. Convection in a porous cavity. *J. Fluid Mechanics*, 1978, **97**, 449–478
11 Bejan, A. On the boundary layer regime in a vertical enclosure filled with a porous medium. *Lett. in Heat Mass Transfer*, 1979, **6**, 93–102
12 Blythe, P. A. and Simpkins, P. G. Convection in a porous layer for a temperature dependent viscosity. *Int. J. Heat Mass Transfer*, 1981, **24**, 497–506
13 Shiralkar, G. S., Haajizadeh, M. and Tien, C. L. Numerical study of high Rayleigh number convection in a vertical porous enclosure. *Numer. Heat Transfer*, 1983, **6**, 223–234
14 Tong, T. W. and Subramanian, E. A boundary-layer analysis for natural convection in vertical porous enclosures—use of Brinkman-extended Darcy model. *Int. J. Heat Mass Transfer*, 1985, **28**, 563–571
15 Tong, T. W. and Subramanian, E. Natural convection in a rectangular enclosure partially filled with a porous medium. *Int. J. Heat Fluid Flow*, 1986, **7**, 3–10
16 Sathe, S. B., Tong, T. W. and Faruque, M. A. An experimental study of natural convection in a partially porous enclosure. *AIAA J. Thermophysics and Heat Transfer*, 1987, **1**, 260–267
17 Beckermann, C., Ramadhyani, S. and Viskanta, R. Natural convection flow and heat transfer between a fluid layer and a porous layer inside a rectangular enclosure. *J. Heat Transfer*, 1986, **109**, 363–370
18 Neale, G. and Nader, W. Practical significance of Brinkman's extension of Darcy law: coupled parallel flows within a channel and a bounding porous medium. *Can. J. Chem. Eng.*, 1974, **52**, 475–478
19 Patankar, S. V. *Numerical Heat Transfer and Fluid Flow*, Hemisphere Publishing Corp., New York, 1980, 90–100
20 Anderson, D. A., Tannehill, J. C. and Pletcher, R. H. *Computational Fluid Mechanics and Heat Transfer*, Hemisphere Publishing Corp., New York, 1984, 39–46
21 Lapidus, L. and Pinder, G. F. *Numerical Solution of Partial Differential Equations in Science and Engineering*, Princeton University Press, New Jersey, 1982, 418–421
22 Roache, P. J. *Computational Fluid Dynamics*, Hermosa, Albuquerque, 1972, 139–171